

Finite Element Analysis of Single Slot Antenna for Microwave Tumor Ablation

Nwoye E.O, Aweda M.A, Oremosu A.A, Anunobi C.C, Akanmu O.N, Ibitoye A.Z, Adeneye S.O, Akpochafor M.O.

College of Medicine, Lagos University Teaching Hospital, Lagos, Nigeria Idi-Araba. P. M. B. 12003 Lagos, Nigerialdi-Araba. P. M. B. 12003 Lagos, Nigeria.

²Department of Biomedical Engineering, College of Medicine, Lagos University Teaching Hospital, Lagos, Nigeria Idi-Araba. P. M. B. 12003 Lagos, Nigeria.

Abstract: This study is aimed at investigating the characteristics of various slot sizes of microwave antenna suitable for ablation of hepatic and other tumors. The single slot antenna for hepatic MWA was designed using COMSOL MULTIPHYSICS 4.3b software. A total number of 140 antennas models were designed out of which one was selected based on the variation in its reflection coefficient, total power density and Specific Absorption Ratio. The three antennas have different geometry parameters based on the effective wavelength in liver tissue at 2.45GHz. The inner and outer conductors of the antenna were modeled using perfect electric conductor (PEC) boundary conditions. The model was simulated at multiple discrete lengths of slot between 2.5mm and 4.5mm, using 0.1mm increment to determine the antenna efficiency. The antenna has a reflection coefficient as low as -44.67618 dB, with a corresponding total power dissipation of 9.47744 W at slot size 3.5 mm. The results show that the antenna operates with low reflection coefficient which at high power levels prevents overheating of the feedline. Feedline overheating may damage the coaxial line, thereby making it is suitable for ablation of hepatic and other tumors.

Keywords: Microwave ablation, Reflection coefficient, Total power dissipation, tumor, Antenna.

I. INTRODUCTION

Microwave ablation (MWA) represents one of the newest generation of thermal ablation technologies; it is increasingly utilized in the treatment of tumor and malignancies. A variety of MWA systems are now clinically available. [1]. Liver cancer is a significant worldwide public health issue. The disease has a mortality rate of 100% at 5 years in untreated cases [2] and results in the deaths of more than one million people each year worldwide [3-6]. Although liver cancer can be treated successfully by surgical resection of the malignant tissue, approximately 90% of patients with the disease are ineligible for the procedure due to factors such as insufficient hepatic reserve and the close proximity of tumors to blood vessels [2, 7]. One promising alternative for these patients is microwave ablation (MWA), an experimental procedure in which an antenna is inserted percutaneously or during surgery [8] to induce cell necrosis through the heating of deep-seated tumors. Microwave technology utilizes energy at frequencies ranging from 915 MHz to 9.2 GHz and differs from other thermal ablation modalities, most notably radiofrequency ablation (RFA), in many key aspects. [9]. Radiofrequency ablation is susceptible to 'heat sink' whereby thermal energy is diverted from the target tissue by the flow of blood through adjacent vessels. [9-14]. The many perceived advantages of microwave ablation have driven researchers to develop innovative antennas to effectively treat deep-seated and nonresectable hepatic tumors. These designs have focused largely on thin, coaxial-based interstitial antennas [15-17], which are minimally invasive and capable of delivering a large amount of electromagnetic power. These antennas can usually be classified as one of three types (dipole, slot, or monopole) based on their physical features and radioactive properties. The propensity of the tissue to be heated in the presence time variable electric field is determined by the values of its electric properties [6], the electric conductivity, and the dielectric permittivity, and other physical properties. The dosimetric quantity that relates to heat generation in tissues is the Specific Absorption Rate (SAR), defined as:

$$SAR = \frac{\sigma E^2}{\rho} \quad 1$$

ρ (kg/m³) represents the mass density of the tissue and E is the (root mean square) (RMS) value of the time harmonic electric field strength inside the exposed tissue. To assist in antenna design for MWA, many researchers have employed the use of mathematical models rooted in computational electromagnetics (CEM), a discipline that employs numerical methods to describe propagation of electromagnetic waves. The finite element method (FEM), has been extensively used in simulations of cardiac and hepatic radio-frequency (RF) ablation [18,19]. FEM models can provide users with quick, accurate solutions to multiple systems of differential

equations and as such, are well suited to heat transfer problems like ablation. Most previous studies of MWA were mainly focused on SAR and did not consider the temperature distribution, reflection coefficient and treatment duration of the antenna. Antennas operating with high reflection coefficients (especially at higher power levels) can cause overheating of the feedline possibly leading to damage to the coaxial line or due to the thin outer conductor damage to the tissue [20].

In this study, the effect of variation of slot sizes on efficiency of antenna for microwave ablation will be systematically studied. The simulated results in this study can be used as a guideline for the practical treatment.

II. METHODS AND MATERIAL

The single slot coaxial antenna is used to transfer microwave power into liver tissue for the treatment of liver cancer. The three modeled antenna has a diameter of 1.79mm each because the thin antenna is required in the interstitial treatments. A ring-shaped slot, 3.4 mm,3.5 mm,3.6 mm wide were cut-off from the outer conductor 5mm in length from the short circuited tip. The effective heating around the tip of the antenna is very important to the interstitial heating because the electric field becomes more stronger near the slot [21]. The antennas are composed of an inner conductor, a dielectric, outer conductor and a metal of width 0.145 mm, 0.325 mm, 0.125 mm and 0.595 mm respectively. The metal is specifically located around the tip of the antenna to increase the heating effect and reflect back the electric field towards the slot. The antennas are enclosed in a catheter of width 0.895 mm (made of polytetrafluorethylene; PTFE), for hygienic and guidance purposes. Fig.1 shows the model geometry of the single slot microwave antenna. The single slot Microwave Antenna operates at the frequency of 2.45GHz, a widely used frequency in MWA, and the input microwave power is varied between 10 W and 50 W. The antenna was simulated by varying the slot height, distance from the tip of the antenna and the metal height using COMSOL Multiphysics 4.3b. The goal of MWA is to elevate the temperature of unwanted tissue to 50°C where cancer cells are destroyed [27]. Dimensions of the antennas are given in Table 1.

TABLE 1. Dimensions of a Microwave Antenna.

Materials	Dimensions (mm)
Inner conductor	0.145
Dielectric	0.325
Outer conductor	0.125
Catheter	0.895
Slot	3.500
Metal	0.595

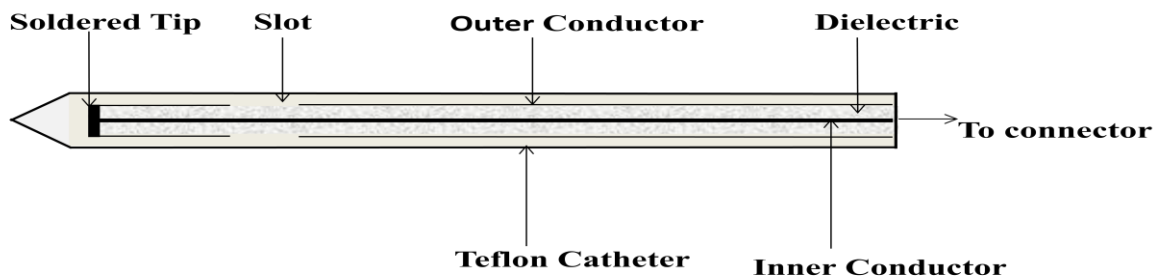


Figure 1: Diagram of the simulated single slot antenna.

The liver tissue is considered as a cylindrical geometry. It has a 30mm radius and 80mm in height. The physical properties of the materials involved in the model are selected from several literatures: Yang et al. [22], Bertram et al. [23], Yang et al. [24] and Jacobsen and Stauffer [25]. The parameters and the values used in the model are given in Table 2 considered at frequency of 2.45GHz.

TABLE 2: The parameters and the values used in the model.

Parameters	Abbreviations	Values
Density of blood	rho_blood	10 ³ [kg/m ³]
Specific heat, blood	Cp_blood	(3639[J/(kg·K)])
Blood perfusion rate	omega_blood	(3.6× 10 ⁻³ 1/s)
Blood temperature	T_blood	(37[°C])
Relative permittivity, liver	eps_liver	43.03

Electric conductivity, liver	sigma_liver	(1.69[S/m])
Thermal conductivity, liver	k_liver	(0.56[W/(m*K)])
Relative permittivity, dielectric	eps_diel	(2.03)
Relative permittivity, catheter	eps_cat	(2.6)
Microwave frequency	F	(2.45[GHz])
Input microwave power	P_in	(10[W])

The model uses a frequency-domain problem formulation with the complex-valued azimuthal component of the magnetic field as the unknown. [28].

III. Domain Boundary Equation - Electromagnetics

An electromagnetic wave propagating in a coaxial cable is characterized by transverse electromagnetic fields (TEM). Assuming time-harmonic fields with complex amplitudes containing the phase information, the appropriate equations are

$$E = e_r \frac{C}{r} e^{j(\omega t - kz)} \tag{2}$$

$$H = e_\phi \frac{C}{rZ} e^{j(\omega t - kz)} \tag{3}$$

$$P_{av} = \int_{r_{inner}}^{r_{outer}} Re \left(\frac{1}{2} E \times H^* \right) 2\pi r dr = e_z \pi \frac{C^2}{Z} \ln \left(\frac{r_{outer}}{r_{inner}} \right) \tag{4}$$

Where z is the direction of propagation, and r , ϕ , and z are cylindrical coordinates centered on the axis of the coaxial cable. P_{av} is the time-averaged power flow in the cable, Z is the wave impedance in the dielectric of the cable, while r_{inner} and r_{outer} are the dielectric's inner and outer radii, respectively. Further, ω denotes the angular frequency. The propagation constant, k , relates to the wavelength in the medium, λ , as

$$k = \frac{2\pi}{\lambda} \tag{5}$$

In the tissue, the electric field also has a finite axial component whereas the magnetic field is purely in the azimuthal direction. Thus, you can model the antenna using an axisymmetric transverse magnetic (TM) formulation. The wave equation then becomes scalar in $H_{\omega 0}$:

$$\nabla \times \left(\left(\epsilon_r - \frac{j\sigma}{\omega\epsilon_0} \right) \nabla \times H_\phi \right)^{-1} - \mu_r k_0^2 H_\phi = 0 \tag{6}$$

The boundary conditions for the metallic surfaces are

$$n \times E = 0 \tag{7}$$

The feed point is modeled using a port boundary condition with a power level set to 10 W. This is essentially a first-order low-reflecting boundary condition with an input field H_ϕ

$$n \times \sqrt{\epsilon} E - \sqrt{\mu} H_\phi = -2 \sqrt{\mu} H_{\phi 0} \tag{8}$$

where

$$H_{\phi 0} = \frac{\sqrt{\frac{P_{av} Z}{\pi r \ln \left(\frac{r_{outer}}{r_{inner}} \right)}}}{r} \tag{9}$$

for an input power of P_{av} deduced from the time-average power flow. The antenna radiates into the tissue where a damped wave propagates. Because you can discretize only a finite region, you must truncate the geometry some distance from the antenna using a similar absorbing boundary condition without excitation. Apply this boundary condition to all exterior boundaries.

Domain And Boundary Equations – Heat Transfer

The bioheat equation describes the stationary heat transfer problem as

$$\nabla \cdot (-k\nabla T) = \rho_b C_b \omega_b (T_b - T) + Q_{met} + Q_{ext} \tag{10}$$

Where k is the liver’s thermal conductivity (W/(m·K)), ρ_b represents the blood density (kg/m³), C_b is the blood’s specific heat capacity (J/(kg·K)), and ω_b denotes the blood perfusion rate (1/s). Further, Q_{met} is the heat source from metabolism, and Q_{ext} is an external heat source, both measured in W/m³. This model neglects the heat source from metabolism. The external heat source is equal to the resistive heat generated by the electromagnetic field:

$$Q_{ext} = \frac{1}{2} Re [(\sigma - j\omega\epsilon) \mathbf{E} \cdot \mathbf{E}^*] \tag{11}$$

The model assumes that the blood perfusion rate is $\omega_b = 0.0036s^{-1}$, and that the blood enters the liver at the body temperature $T_b=37$ °C and is heated to a temperature, T . The blood’s specific heat capacity is $C_b=3639$ J/(kg·K). At least for external body parts such as hands and feet, it is evident that a temperature increase results in an increased blood flow. This example models the heat-transfer problem only in the liver domain. Where this domain is truncated, it uses insulation, that is

$$\mathbf{n} \cdot \nabla T = 0 \tag{12}$$

IV. Results

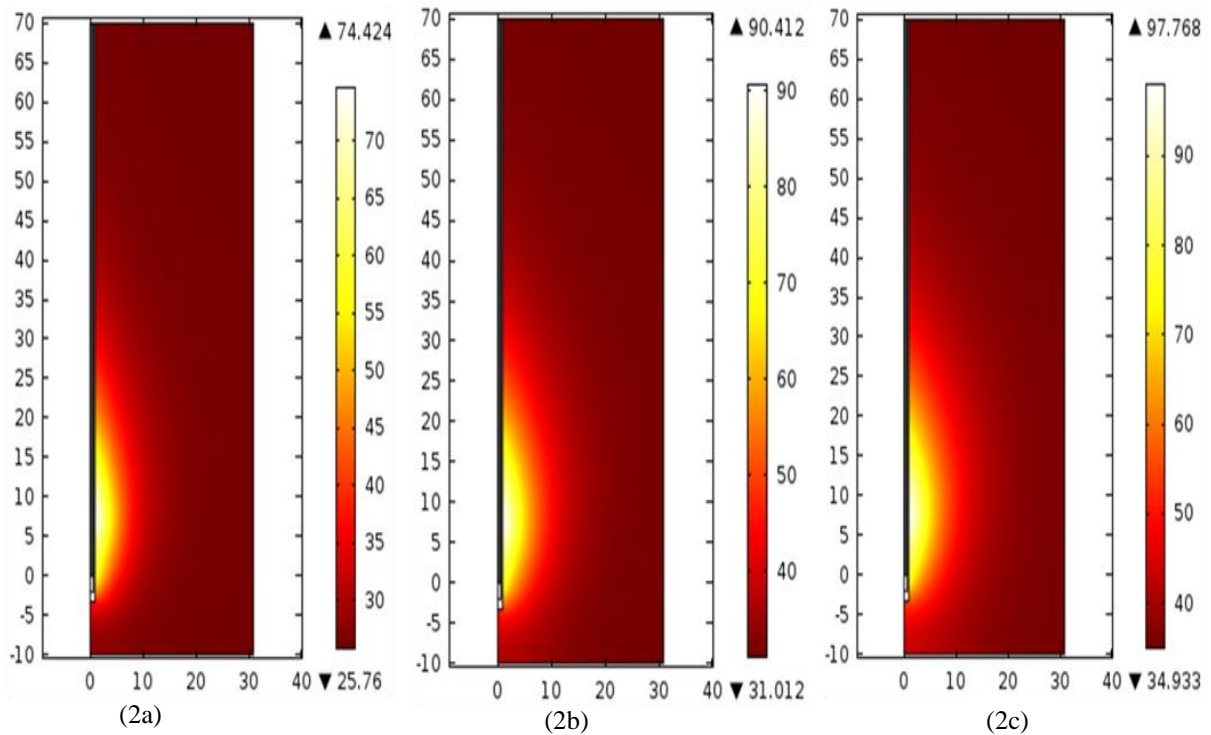


Figure 2(a)(b)(c): The resulting steady-state axisymmetric temperature distribution for durations of 120s, 300s and 600s in the liver tissue.

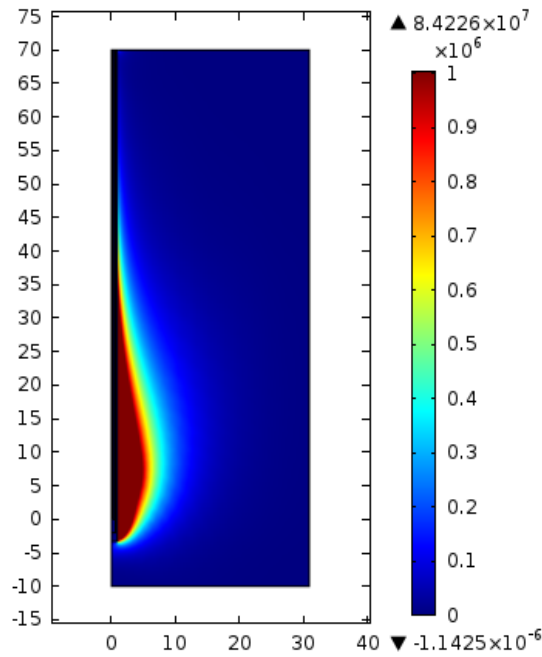


Figure 3: The computed microwave heat-source density takes on its highest values near the tip and the slot. The scale is cut off at 1 W/cm³.

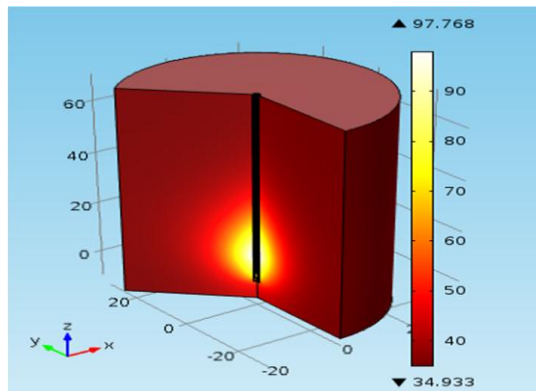


Figure 4: The 3D Plot of the temperature distribution on the liver tissue at 600s.

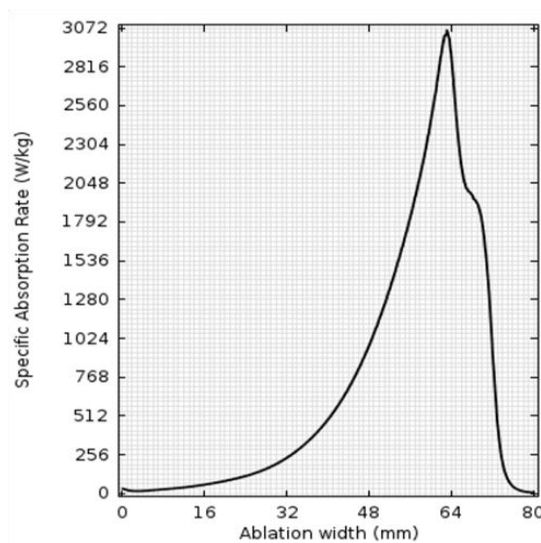


Figure 5: The SAR distribution along a line parallel to the antenna.

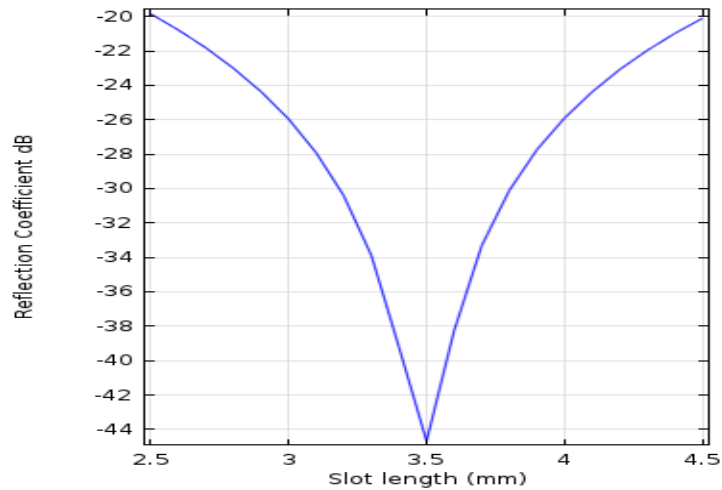


FIGURE 6: The simulated single slot antenna with reflection coefficient, -44.67618 dB, at slot Size 3.5 mm.

TABLE 4: Result of the measured ablation diameter with time at different power and at 50°C for 3.5 mm slot antenna design.

Time (s)	Ablation diameter (mm) at different powers				
	10 W	20 W	30 W	40 W	50 W
60	2.4	10.8	13.6	15.5	17.3
120	6.4	15.8	19.2	21.7	23.7
180	8.7	19.2	23.1	25.8	28.0
240	10.2	21.8	26.0	29.0	31.4
300	11.5	24.0	28.4	31.5	34.0
360	12.5	25.8	30.3	33.5	36.2
420	13.2	27.2	31.9	35.3	37.8
480	13.8	28.2	32.3	36.8	39.8
540	14.3	29.2	34.2	37.6	40.6
600	14.8	30.0	35.0	38.8	41.6

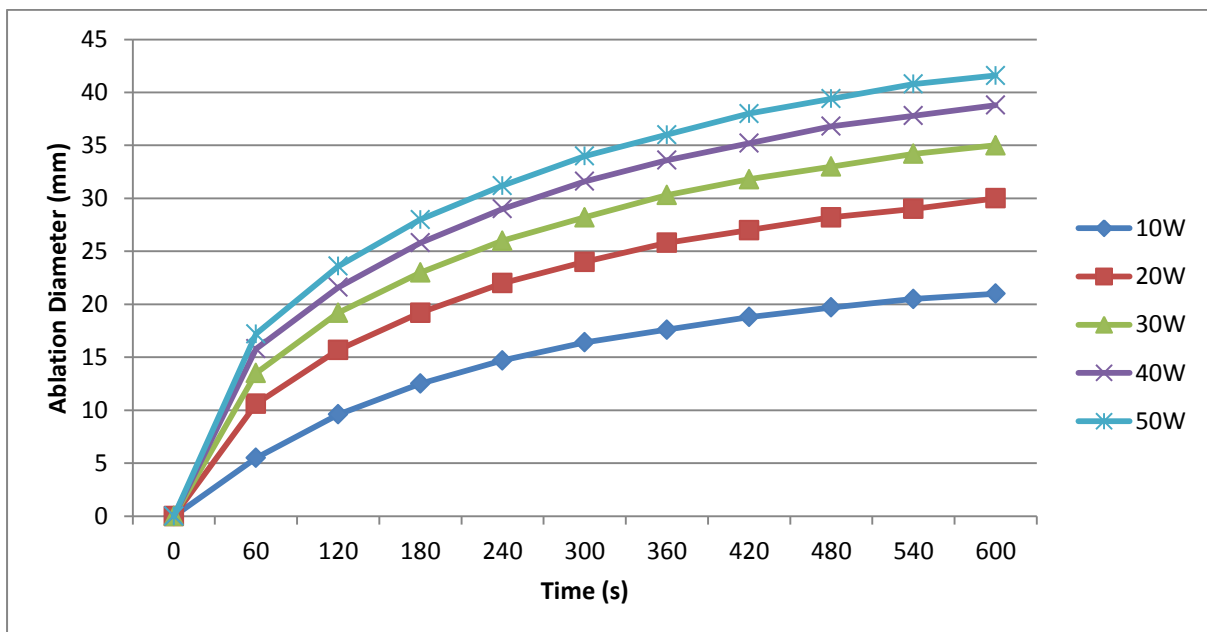


FIGURE 7: Comparison of ablation diameter with time at different power for 3.5mm slot antenna design.

V. Discussion

Figure 2(a)(b)(c) shows the resulting steady-state axisymmetric temperature distribution for durations of 120s, 300s and 600s in the liver tissue for an input microwave power of 10 W. The temperature distribution is near ellipsoidal distribution around the slot and its highest values near the microwave antenna slot. It then decreases with distance from the antenna and reaches 25.76 °C, 31.012 °C and 34.933 °C closer to the outer boundaries of the computational domain. The perfusion of relatively cold blood seems to limit the extent of the area that is heated. In addition, temperature distribution increases with increasing time. This is because the microwave power absorbed within the liver tissue attenuates, owing to energy absorption, and thereafter the absorbed energy is converted into thermal energy which increases the liver temperature. The maximum temperature within the liver tissue at time 120 s, 300 s, 600s are 74.424 °C, 90.412 °C and 97.768 °C which is quite lower to the ones simulated by P. Keagin et al., 2011.

Table 3 shows the computer-simulated results of microwave power absorbed in the liver tissues base on a frequency of 2.45 GHz and a microwave power of 10 W. Figure 3 illustrates the volume heating effect expected from MWA. Microwaves power emitted from the MCA (Microwave coaxial antenna) propagates through the liver tissue, which is converted to heat by dielectric heating. [29]. Figure 3 also shows the axisymmetric distribution of the microwave heat source. Clearly the temperature field follows the heat-source distribution quite well. That is, near the antenna the heat source is strong, which leads to high temperatures, while far from the antenna, the heat source is weaker and the blood manages to keep the tissue at normal body temperature. Figure 4 shows the 3D Plot of the temperature distribution on the liver tissue at 600s.

Figure 5 plots the specific absorption rate (SAR) along a line parallel to the antenna. The results are in good agreement with those found by K. saito et al., 2000. For the treatment of deep-seated hepatic tumors, the SAR patterns of an interstitial antenna should be highly localized near the distal tip of the antenna [23] which is clearly shown in figure 5.

Figure 6 shows the simulated single slot antenna at a 2.45 GHz MWA frequency with reflection coefficient, -44.67618 dB, at slot length 3.5 mm which is lower than the antenna simulated by John M Bertam et al., 2006. The frequency where the reflection coefficient is minimal is commonly referred to as the resonant frequency and should be approximately the same as the operating frequency of the generator used [23]. Antennas operating with high reflection coefficients (table 3) (especially at higher power levels) can cause overheating of the feedline possibly leading to damage to the coaxial line or due to the thin outer conductor damage to the tissue [26].

Figure 7 shows the comparison of ablation diameter with time at different power for 3.5mm slot antenna design. This antenna was selected because it has the lowest reflection coefficient. One of the main challenges of MWA is the ablation area covered. The goal of MWA is to elevate the temperature of unwanted tissue to 50°C where cancer cells are destroyed [27]. In this work, we discovered that the ablation width increases as the power is increased per time. According to David M. Lloyd et al. 2011, 114 patients were treated with MWA and median size of ablated lesions was 2.5cm (range 0.5-9.5 cm) with a power setting of 100W. This shows that the antenna designed in this work is more efficient in terms of the power usage and has a high ablation width of 4.16cm which is quite wider than the results obtained by David M. Lloyd et al 2011.

VI. Conclusion

The result shows that the antennas operate with low reflection coefficients of - 44.67618 dB which at high power levels prevents overheating of the feedline which leads to damage of the coaxial line, therefore it is suitable for ablation of hepatic and other tumors. In this work, single slot microwave antenna for interstitial MWA in liver is evaluated and it is shown that variation in the slot size of the antenna model has an effect on the microwave power absorbed, reflection coefficient, SAR distribution and temperature distribution in the liver tissue. It is also found that single slot antenna can be used to obtain a larger ablation depth with lower power and temperature.

References

- [1]. International multicenter prospective study on microwave ablation of liver tumours: preliminary results. David M. Lloyd1, Kwan N. Lau, Fenella Welsh, Kit-Fai Lee, David J. Sherlock, Michael A. Choti, John B. Martinie & David A. Iannitti. International Microwave Tumour Ablation Group (IMTAG). OI:10.1111/j.1477-2574.2011.00338.
- [2]. McGahan JP, Dodd GD: Radiofrequency ablation of the liver: Current status. Am J Roentgenol2001, 176:3-16.
- [3]. Chinn SB, Lee FT, Kennedy GD, Chinn C, Johnson CD, Winter TC, Warner TF, Mahvi DM: Effect of vascular occlusion on radiofrequency ablation of the liver: Results in a porcine model. Am J Roentgenol176, 2001.:789-795.
- [4]. Haemmerich D, Staelin ST, Tungjitkusolmun S, Lee FT, Mahvi DM, Webster JG: Hepatic bipolar radio-frequency ablation between separated multiprong electrodes. IEEE Trans Biomed Eng2001, 48:1145-1152.
- [5]. Lau WY, Leung TWT, Yu SCH, Ho SKW: Percutaneous local ablative therapy for hepatocellular carcinoma - A review and look into the future. Ann Surg 237:2003, 171-179.
- [6]. Wright AS, Mahvi DM, Haemmerich DG, Lee FTJ: Minimally invasive approaches in management of hepatic tumors. SurgTechnolInt11:2003, 144-153.

- [7]. Cha C, Lee FT: Rationale for the combination of cryoablation with surgical resection of hepatic tumors. *Journal of Gastrointestinal Surgery* 5: 2001, 206-213.
- [8]. Wright AS, Lee FT, Mahvi DM: Hepatic microwave ablation with multiple antennae results in synergistically larger zones of coagulation necrosis. *Ann SurgOncol*10:2003, 275-283.
- [9]. Brace CL. Radiofrequency and microwave ablation of the liver, lung, kidney, and bone: what are the differences? *CurrProblDiagnRadiol*38:2009135–143.
- [10]. S.N. Goldberg, G.S Gazelle. L. Solbratt. W.J Rittman and P.R Mueller, “Radiofrequency tissue ablation increased lesion diameter with a perfusion electrode”.*Acad. Radiol.*. vol. 3, August 1996, pp. 636-44,.
- [11]. Kim SK, Rhim H, Kim YS, Koh BH, Cho OK, Seo HS et al. Radiofrequency thermal ablation of hepatic tumours: pitfalls and challenges. *Abdom Imaging* 30:(2005) 727–733.
- [12]. Patterson EJ, Scudamore CH, Owen DA, Nagy AG, Buczkowski AK. Radiofrequency ablation of porcine liver in vivo: effects of blood flow and treatment time on lesion size. *Ann Surg*227:(1998) 559–565.
- [13]. Lu DS, Raman SS, Limanond P, Aziz D, Economou J, Busuttill R et al. Influence of large peritumoral vessels on outcome of radiofrequency ablation of liver tumours. *J VascIntervRadiol*14:(2003)1267–1274.
- [14]. Wright AS, Sampson LA, Warner TF, Mahvi DM, Lee FT Jr. Radiofrequency versus microwave ablation in a hepatic porcine model. *Radiology* 236:(2005)132–139.
- [15]. Schaller G, Erb J, Engelbrecht R: Field simulation of dipole antennas for interstitial microwave hyperthermia. *IEEE Trans Microwave Theory Tech*1996, 44:887-895.
- [16]. Longo I, Gentili GB, Cerretelli M, Tosoratti N: A coaxial antenna with miniaturized choke for minimally invasive interstitial heating. *IEEE Trans Biomed Eng*2003, 50:82-88.
- [17]. Brace CL, van der Weide DW, Lee FT, Laeseke PF, Sampson LA: Analysis and experimental validation of a triaxial antenna for microwave tumor ablation. *MicrowSymp Dig 2004 IEEE MTT-S Int*2004, 3:1437-1440.
- [18]. Tungjitkusolmun S, Staelin ST, Haemmerich D, Tsai JZ, Cao H, Webster JG, Lee FT, Mahvi DM, Vorperian VR: Three-dimensional finite-element analyses for radio-frequency hepatic tumor ablation. *IEEE Trans Biomed Eng*2002, 49:3-9.
- [19]. Haemmerich D, Chachati L, Wright AS, Mahvi DM, Lee FT, Webster JG: Hepatic radiofrequency ablation with internally cooled probes: Effect of coolant temperature on lesion size. *IEEE Trans Biomed Eng*2003, 50:493-500.
- [20]. Nevels RD, Arndt GD, Raffoul GW, Carl JR, Pacifico A: Microwave catheter design. *IEEE Trans Biomed Eng*1998, 45:885-890.
- [21]. K. Saito, Y. Hayashi, H. Yoshimura, K. Ito, Heating characteristics of array applicator composed of two coaxial-slot antennas for microwave coagulation therapy, *IEE Transactions on Microwave Theory and Techniques* 48 (2000) 1800-1806 (I PART 1).
- [22]. D.Yang, M. Converse, D. Mahvi, Expanding the bioheat equation to include tissue internal water evaporation during heating, *IEEE Transactions on Biomedical Engineering* 54 (8) (2007) 1382-1388.
- [23]. J.M. Bertram, D.Yang, M.C. Converse, Antenna design for microwave hepatic ablation using an axisymmetric electromagnetic model, *Biomedical Engineering Online* 5 (2006).
- [24]. D. Yang, J.M. Bertram, M.C. Converse, et al., A floating sleeveantenna yields localized hepatic microwave ablation, *IEEE Transactions on Biomedical Engineering* 53 (3) (2006) 533-537.
- [25]. S. Jacobsen, P.R. Stauffer, Can we settle with single-band radiometric temperature monitoring during hyperthermia treatment of chestwall recurrence of breast cancer using a dual-mode transceiving applicator? *Physics in Medicine and Biology* 52 (4) (2007) 911-928.
- [26]. Nevels RD, Arndt GD, Raffoul GW, Carl JR, Pacifico A: Microwave catheter design. *IEEE Trans Biomed Eng*1998, 45:885-890.
- [27]. J.P. McGahan, J.M. Brock, H. Tesluk, W.Z. Gu, P. Schneider, P.D. Browning, Hepatic ablation with use of radio-frequency electrocautery in the animal model, *journal of Vascular and interventional Radiology : JVIR* 3 (2) (1992) 291-297.
- [28]. COMSOL Multiphysics™, v.4.3b. (2013). Users' Guide. Electromagnetic Module, Heat Transfer Module.
- [29]. P. Keangin, P. Rattanadecho, T. Wessapan, An analysis of heat transfer in liver tissue during microwave ablation using single and double slot antenna. *ICHMT – 02354*, Elsevier 2011.